ZYS-1 is not an ADAR1 inhibitor

Cassandra N. Smoak[1], Estelle N. Gardner[1], Renee N. Chua[1], Kyle A. Cottrell [1,2]

[1]Department of Biochemistry, Purdue University, West Lafayette, IN, USA

[2]Purdue Institute for Cancer Research, Purdue University, West Lafayette, IN, USA

The authors declare no potential conflicts of interest.

Correspondence:

Kyle A Cottrell, Ph.D.
Department of Biochemistry
Purdue University
201 S University St.
West Lafayette, IN
Email: kacottre@pudue.edu
Telephone: 765-494-6941

Shortened title: ZYS-1 is not an ADAR1 inhibitor

Keywords: ADAR1, cancer, RNA

Abstract

Adenosine deaminase acting on RNA 1 (ADAR1) edits double-stranded RNA (dsRNA) substrates by the deamination of adenosine to inosine in a process known as A-to-I editing. Modulation of ADAR1 expression and editing activity has previously been described to play a role in cancer development and progression, with upregulation of ADAR1 being observed in a range of cancers. Further, depletion of ADAR1 leads to increased sensing of endogenous dsRNAs by dsRNA sensors in cell lines that require ADAR1 for survival, which are termed ADAR1-dependent. The activation of these sensors induces downstream production of type I interferons as well as translational inhibition and apoptosis. Therefore, ADAR1 is a promising oncologic therapeutic target. Recently, the small molecule ZYS-1 has been developed and presented as a direct inhibitor of ADAR1. We performed a series of in vitro and cellular experiments to validate the efficacy and specificity of ZYS-1 as an ADAR1 inhibitor. Evaluating the effect of ZYS-1 on cell viability revealed it to be equally cytotoxic to both ADAR1-dependent and ADAR1-independent cell lines, as well as wildtype and ADAR1 knockout cells. Moreover, ZYS-1 treatment had little effect on activation of PKR or induction of IFN stimulated genes. Importantly, treatment with ZYS-1 did not reduce cellular A-to-I editing for several known ADAR1 editing sites, and did not inhibit in vitro A-to-I editing by recombinant ADAR1. Together, these data indicate that ZYS-1 is not a selective inhibitor of ADAR1.

41 **Introduction**

42 The RNA editing enzyme ADAR1 is an important regulator of double-stranded RNA
43 (dsRNA) sensing pathways (Cottrell et al. 2024a; Heraud-Farlow and Walkley 2020).
44 Adenosine-to-inosine (A-to-I) editing by ADAR1 prevents activation of MDA5 by endogenous
45 dsRNAs (Liddicoat et al. 2015; Pestal et al. 2015; Mannion et al. 2014). Additionally, ADAR1
46 suppresses activation of the dsRNA sensor PKR in an RNA editing-independent manner
47 (Sinigaglia et al. 2024; Chung et al. 2018; Hu et al. 2023). These functions of ADAR1 are
48 essential in embryonic development and, importantly, in many cancer cell lines (Wang et al.
49 2004; Hartner et al. 2004; Gannon et al. 2018; Liu et al. 2019; Kung et al. 2021). Depletion of
50 ADAR1 in roughly half of cancer cells causes cell death (Liu et al. 2019; Gannon et al. 2018;
51 Kung et al. 2021). In these ADAR1-dependent cells, depletion of ADAR1 causes activation of
52 PKR – which drives cell death – and activation of MDA5 leading to type I interferon signaling
53 and expression of IFN-stimulated genes (ISGs). The IFN response caused by ADAR1 knockout
54 can overcome resistance to immune checkpoint blockade (Ishizuka et al. 2019). These
55 phenotypes associated with ADAR1 depletion make ADAR1 an important therapeutic target for
56 many cancers, especially those with poor response to immune checkpoint blockade. However,
57 there are currently no FDA-approved ADAR1 inhibitors.

58 The substrate of ADAR1 is an adenosine residue within duplexed RNA (Bass and
59 Weintraub 1988; Wagner and Nishikura 1988). While the modified adenosine can either be
60 base-paired or not (Wong et al. 2001), ADAR1 has no activity on single-stranded RNA (Bass
61 and Weintraub 1988; Wagner and Nishikura 1988), or on adenosine or adenine alone (Polson et
62 al. 1991). Previously, two small molecule adenosine analogues have been reported to disrupt
63 ADAR1 function – 8-azaadenosine (Ramírez-Moya et al. 2020; Zipeto et al. 2016) and 8-
64 chloroadenosine (Ding et al. 2020) – however, through extensive evaluation, we found that
65 neither are selective inhibitors of ADAR1 (Cottrell et al. 2021). Recently, ZYS-1, another
66 adenosine analogue (Figure 1a), has been reported to inhibit ADAR1(Wang et al. 2025) and has

67 been used in subsequent studies (Shi et al. 2025). Here we carefully evaluate the efficacy and
68 specificity of ZYS-1 as an ADAR1 inhibitor. Through a series of cellular and in vitro experiments,
69 we found no evidence supporting ZYS-1 as an ADAR1 inhibitor.

70 **Results**

71 **ZYS-1 is broadly cytotoxic**

72 A selective inhibitor of ADAR1 would be expected to be more cytotoxic towards ADAR1-
73 dependent cell lines than ADAR1-independent lines. As such, we evaluated the effect of ZYS-1
74 treatment on cell viability in a panel of ADAR1-dependent and ADAR1-independent cell lines.
75 We chose two dependent cell lines (HCC1806 and MDA-MB-468) and two independent cell
76 lines (BT-549 and MDA-MB-453) based on either DepMap data (Broad 2024) (Fig. 1b) or our
77 previous studies (Kung et al. 2021). Irrespective of the ADAR1-dependency status, ZYS-1 was
78 strongly cytotoxic towards all cell lines evaluated (Fig. 1c). As measured by an ATP-dependent
79 luciferase-based assay for cell viability, we found the EC50 of ZYS-1 to vary little across the cell
80 lines in our panel and to be lowest in the ADAR1-independent cell line BT-549. Crystal violet
81 staining of cells treated with ZYS-1 supported the robust toxicity of ZYS-1 (Figure 1d-e).

82 To more rigorously evaluate the specificity of ZYS-1, we assessed its effect on cell
83 viability in WT and ADAR1 knockout (ADAR1-KO) BT-549 (Fig. 1f). The EC50 for ZYS-1 in WT
84 and ADAR1-KO BT-549 cells was nearly identical (0.14 and 0.12 μM, respectively (Fig. 1g)).
85 Importantly, the WT and ADAR1-KO BT-549 were equally viable in the absence of ZYS-1
86 (Supplemental Figure 1a). We attempted to assess the effect of ZYS-1 by crystal violet staining,
87 but found that ADAR1-KO BT-549 cells detached easily during the staining process
88 (Supplemental Fig. S1b). Together with the results above, these data strongly indicate that ZYS-
89 1 does not cause cell death by affecting ADAR1.

90 **ZYS-1 does not phenocopy ADAR1 depletion**

91 Depletion of ADAR1 in ADAR1-dependent cells produces a viral mimicry phenotype that
92 includes activation of PKR (indicated by autophosphorylation on Thr446 (Romano et al. 1998))

93 and MDA5, with the latter driving a type I IFN response (Liu et al. 2019; Gannon et al. 2018).
94 Both of these phenotypes were observed upon ZYS-1 treatment in the original study reporting
95 ZYS-1 as an ADAR1 inhibitor (Wang et al. 2025). We evaluated the effect of ZYS-1 on PKR
96 activation and ISG induction using two ADAR1-dependent cell lines that we have previously
97 studied (Cottrell et al. 2021; Kung et al. 2021). ZYS-1 treatment of the ADAR1-dependent cell
98 lines HCC1806 and MDA-MB-468 had no effect on PKR activation (Fig. 2a-b). Previously ZYS-1
99 has been shown to reduce ADAR1 expression (Wang et al. 2025), however, we observed no
100 change in ADAR1 expression in ZYS-1-treated HCC1806 and MDA-MB-468 (Fig. 2a and Fig.
101 2c). Increased expression of ISGs is a phenotype of ADAR1 depletion in ADAR1-dependent
102 cancer cell lines (Cottrell et al. 2021; Liu et al. 2019). We evaluated the expression of four ISGs
103 in ZYS-1-treated HCC1806 and MDA-MB-468. ZYS-1 did not affect ISG expression in HCC1806
104 and caused elevated expression of only one ISG in MDA-MB-468 (Fig. 2d). Together with our
105 evaluation of PKR activation, these data strongly indicate that ZYS-1 does not phenocopy
106 ADAR1 depletion.

107 **ZYS-1 does not inhibit A-to-I editing**

108 A-to-I editing by ADAR1 can be easily evaluated by sequencing of cDNA. Since inosine
109 more readily base-pairs with cytidine, cDNA made from an edited RNA will have a guanosine at
110 the editing site (for the sense strand of duplex cDNA or a cytidine on the anti-sense strand).
111 Sanger sequencing is routinely used to evaluate the level of editing at a given site by comparing
112 the peak heights of A or G (T or C on the antisense stand). We used this approach to evaluate
113 the effect of ZYS-1 treatment on A-to-I editing in cells and in vitro using purified ADAR1 and a
114 well-characterized substrate RNA. For editing in cells, we evaluated editing at three previously
115 characterized editing sites. Editing at all three sites was greatly reduced by knockdown of
116 ADAR1 in HCC1806 (Fig. 3a-b, Supplemental Figure S2). In ZYS-1-treated cells, editing was
117 either not affected or increased for all but one site (Fig. 3c-h). For an editing site in the gene
118 ZDHHC20, we observed significantly reduced editing at the highest concentration of ZYS-1

119 used in BT-549, but not in the other cell lines evaluated. It should be noted that this reduced
120 editing occurred with 1 μM ZYS-1 treatment – a dose that is an order of magnitude higher than
121 the EC50 for cell viability in this cell line.

122 Since it is known that other proteins can regulate A-to-I editing at specific sites (Hong et
123 al. 2018; Freund et al. 2020), it is possible that some changes in editing observed in cells upon
124 ZYS-1 treatment could be the result of off-target effects. To evaluate direct inhibition of ADAR1,
125 we performed an in vitro A-to-I editing assay with purified ADAR1 and an *in vitro* transcribed
126 RNA containing a portion of the mRNA coding for 5-hydroxytryptamine receptor 2C (5-HT_{2C},
127 encoded by *HTR2C*). The 5-HT_{2C} mRNA contains a well-characterized ADAR1 editing site,
128 known as the 'B-site', and is frequently used in A-to-I editing assays (Burns et al. 1997). The 5-
129 HT_{2C} B-site was well edited by ADAR1 in DMSO controls (Fig. 3i-j), though we observed
130 differences in editing based on the lot of ADAR1 used (see Supplemental Fig. S3 for additional
131 data from a different enzyme lot and additional assay controls). Addition of ZYS-1 to the editing
132 assay had no effect on A-to-I editing at any dose used (Fig. 3i-j and Supplemental Fig. S3a-b).
133 Together with the cellular A-to-I editing data above, these data indicate that ZYS-1 is not an
134 ADAR1 inhibitor.

135 **Discussion**

136 Many studies have now shown the therapeutic potential of targeting ADAR1 to treat a
137 range of cancers (Liu et al. 2019; Ishizuka et al. 2019; Gannon et al. 2018; Kung et al. 2021). In
138 addition to the cell-intrinsic effects of disrupting ADAR1, the cell-extrinsic effects, such as
139 overcoming resistance to immune checkpoint blockade, strengthen the potential of therapies
140 targeting ADAR1. As such, identifying small molecule inhibitors of ADAR1 is of great
141 importance. Previously reported ADAR1 inhibitors, the adenosine analogues 8-azaadenosine
142 and 8-chloroadenosine, have not proven to be effective in subsequent studies (Cottrell et al.
143 2021). Unfortunately, our data above indicate that the adenosine analogue ZYS-1 is not a
144 selective inhibitor of ADAR1.

145 While we show that ZYS-1 effectively kills many breast cancer cell lines, it does so not
146 by inhibiting ADAR1. Our data are very different from those reported in the initial publication
147 describing ZYS-1 as an ADAR1 inhibitor (Wang et al. 2025). There are a few possible
148 explanations for the differences between these studies. First, the original paper reporting ZYS-1
149 as an ADAR1 inhibitor, Wang et al., 2025, used a commercial assay for Adenosine Deaminase
150 (ADA) to assess inhibition of A-to-I editing by ADAR1 (Wang et al. 2025). That assay is not
151 designed to assess ADAR1 activity and has been reported to be incapable of detecting A-to-I
152 editing (Zhang et al. 2025). Here we used a conventional in vitro A-to-I editing assay to evaluate
153 inhibition of ADAR1 by ZYS-1 and observed no inhibition, consistent with the findings of a
154 recent preprint (Zhang et al. 2025). Second, while Wang et al., 2025 provided evidence that
155 ZYS-1 inhibited A-to-I editing within cells, they evaluated only one editing site in two cell lines.
156 We evaluated three editing sites across four cell lines and observed a significant editing
157 reduction at only one site, in one cell line. Most sites had no observable change, and we even
158 found some sites to have increased editing. Because A-to-I editing by ADAR1 can be regulated
159 by other proteins (Freund et al. 2020; Hong et al. 2018), it is possible that a small molecule
160 could indirectly affect A-to-I editing, which could explain both increased or decreased editing at
161 specific sites. Third, in Wang et al., 2025, the authors evaluated the effect of ZYS-1 on cell
162 viability in control and ADAR1 knockout cell lines. They found ZYS-1 to be less effective in the
163 ADAR1 knockout cells. However, in that experiment, knockout of ADAR1 greatly reduced cell
164 viability, which could have reduced the efficacy of ZYS-1 (which we suspect is inhibiting DNA
165 synthesis, see below). In contrast, we performed a similar experiment with control versus
166 ADAR1 knockout cells, using an ADAR1-independent cell line to ensure that knockout did not
167 affect cell viability. In our experiment, ZYS-1 efficacy was not affected by ADAR1 knockout.
168 While ZYS-1 is not a selective ADAR1 inhibitor, it is highly cytotoxic to cancer cells.
169 ZYS-1 is a derivative of fludarabine. Fludarabine has a long history as a chemotherapeutic used
170 for multiple leukemias and lymphomas (Gandhi and Plunkett 2002). Its mechanism of action

171 involves inhibition of DNA synthesis, through both inhibition of DNA polymerase and
172 ribonucleotide reductase (Gandhi and Plunkett 2002). We suspect that ZYS-1 is functioning
173 through the same mechanism. This would explain its cytotoxicity.

174 Finally, it is our opinion that adenosine analogues are unlikely to inhibit ADAR1 (or
175 ADAR2). Early studies demonstrated that ADAR1 is highly selective for dsRNA(Bass and
176 Weintraub 1988; Wagner and Nishikura 1988; Polson et al. 1991). Unlike ADA, ADAR1 cannot
177 be inhibited by coformycin or 8-azanebularine – both of which structurally resemble the hydrated
178 reaction intermediate of the adenosine deamination reaction (Polson et al. 1991; Mendoza et al.
179 2023). However, when incorporated into a duplexed RNA, but not single-stranded RNA, 8-
180 azanebularine potently inhibits ADAR1 with a low nanomolar IC50 (Mendoza et al. 2023). These
181 findings suggest that additional interactions between ADAR1 and the substrate dsRNA are
182 required to adjust the conformation of the active site and allow binding to adenosine – a model
183 that was first suggested over three decades ago (Polson et al. 1991). This model is supported
184 by structural studies of ADAR1 and ADAR2 indicating multiple interactions between active site
185 adjacent residues and either the phosphodiester backbone of the dsRNA substrate or the
186 'orphan' base opposite the edited adenosine (Fisher and Beal 2024; Matthews et al. 2016; Deng
187 et al. 2025). For ADAR2, the interactions between the deaminase domain and the dsRNA
188 substrate cause long-distance changes to the deaminase domain structure (Matthews et al.
189 2016). These prior observations, along with our evaluation of ZYS-1 and other adenosine
190 analogues (Cottrell et al. 2021), all indicate that selective inhibition of ADAR1 is unlikely to be
191 accomplished via an adenosine analogue.

192 **Materials and Methods**

193 **Cell Culture and Lentiviral Transduction**

194 The cell lines (HEK293T (RRID: CVCL_0063), MDA-MB-453 (RRID: CVCL _0418),
195 MDA-MB-468 (RRID: CVCL_0063), BT-549 (RRID: CVCL_1092), and HCC1806 (RRID:
196 CVCL_1258)) were purchased from the American Type Culture Collection and cultured as

197 described previously (Young et al. 2025). Detailed methods are provided in the Supplemental
198 Information. For some experiments we used the above cell lines engineered for inducible
199 expression of Cas9. These iCas9 cell lines were described previously by our laboratory (Young
200 et al. 2025). The iCas9 lines were used for ADAR1 knockout (Fig. 1e-f, BT-549 iCas9) and for
201 evaluating ZYS-1 efficacy in the cell lines MDA-MB-453 and MDA-MB-468. ZYS-1 (Fludarabine-
202 Cl) was purchased from MedChemExpress (Cat# HY-145443).
203 Lentiviral production and transduction was performed as described previously (Young et
204 al. 2025). Detailed methods are provided in the Supplemental Information.
205 **Plasmids**
206 Oligos encoding an ADAR1-targeting sgRNA (Table S1) were cloned into lenti-sgRNA-
207 hygro (a gift from Brett Stringer (Stringer et al. 2019), Addgene #104991;
208 RRID:Addgene_104991) by ligating annealed and phosphorylated oligos into a digested and
209 dephosphorylated vector. The lenti-sgC1-hygro, generated previously (Young et al. 2025),
210 expresses a control sgRNA that targets a control genomic locus (AAVS1) and has been used
211 previously (Zou et al. 2024; Young et al. 2025). The ADAR1 sgRNA used is from the Avana
212 library used in DepMap (Broad 2024).
213 The control and ADAR1 knockdown plasmids (tet-pLKO-shSCR-puro-luc and tet-pLKO-
214 shADAR1-puro-luc) were generated by cloning of oligonucleotides encoding either shSCR or
215 shADAR1 into the plasmid tet-pLKO-puro-luc by ligating annealed and phosphorylated oligos
216 into a digested and dephosphorylated vector, see Supplemental Information for oligonucleotide
217 sequences. To generate tet-pLKO-puro-luc, first a PstI site was inserted at the end of PuroR in
218 tet-pLKO-puro (a gift from Dmitri Wiederschain (Wiederschain et al. 2009), Addgene plasmid #
219 21915, RRID:Addgene_21915) by site directed mutagenesis using PrimeSTAR Max DNA
220 Polymerase (Takara Bio) and In-Fusion Snap Assembly (Takara). A region of the plasmid
221 pRG01-U6-DR-crRNA-BsmbI(x2)-6T; EFS-Puro-2A-Fluc-WPRE (a gift from Sidi Chen (Chow et
222 al. 2019), Addgene plasmid # 123362, RRID:Addgene_123362) encoding PuroR-2A-Fluc was

223 PCR amplified and digested with BsiWI and PstI prior to ligation into the tet-pLKO-puro-PstI
224 digested with the same enzymes. See Supplemental Table 1 for all primer sequences. Both the
225 control and ADAR1 targeting shRNAs used here have been used previously to evaluate ADAR1
226 function in breast cancer (Kung et al. 2025; Kung et al. 2021; Young et al. 2025; Cottrell et al.
227 2024b; Cottrell et al. 2021). The sequences for both shRNAs are listed in Table S1.
228 All plasmids were confirmed by Sanger sequencing and Nanopore whole plasmid
229 sequencing as well as restriction enzyme digestion.

230 **Genetic Depletion by CRISPR-Cas9 or RNAi**

231 To generate ADAR1 knockout in BT-549, BT-549 iCas9 cell lines were transduced with
232 lentivirus made with lenti-sgADAR1-hygro or lenti-sgC1-hygro and selected with hygromycin.
233 The cells were treated with 2 μg/mL doxycycline to induce Cas9 expression for at least seven
234 days prior to maintenance in media without doxycycline for at least three days before
235 experimentation. To establish the BT-549 ADAR1 knockout cell line, we screened clonal lines
236 for ADAR1 knockout by immunoblot. We used the polyclonal sgC1 line as our control.
237 For knockdown of ADAR1, HCC1806 cells were transduced with either tet-pLKO-
238 shSCR-puro-luc or tet-pLKO-shADAR1-puro-luc and selected with puromycin. Knockdown of
239 ADAR1 was initiated by doxycycline treatment at 2 μg/mL.

240 **Immunoblot**

241 Immunoblot analysis was performed as previously described, with between 25 and 40
242 micrograms of protein loaded per lane (Young et al. 2025). Detailed methods are described in
243 the Supplemental Information. For ZYS-1-treated cells, cells were treated with DMSO or ZYS-1
244 for 48 hours prior to harvesting protein. Primary antibodies used include: ADAR1 (Santa Cruz
245 Biotechnology Cat# sc-73408, RRID:AB_2222767), PKR (Cell Signaling Technology Cat# 3072,
246 RRID:AB_2277600), PKR Thr-446-P (Abcam Cat# ab32036, RRID:AB_777310), GAPDH
247 (Santa Cruz Biotechnology Cat# sc-47724, RRID:AB_627678), and beta-tubulin (Abcam Cat#
248 ab6046, RRID:AB_2210370).

249 **Cell Viability and Proliferation Assessment**

250 To assess cell viability, 2,500 (HCC1806 and BT-549) or 5,000 (MDA-MB-453 and MDA-
251 MB-468) cells were plated in triplicate per condition in 96-well plates. The cells were treated as
252 indicated one day after plating. CellTiter-Glo 2.0 (Promega) was used to determine cell viability
253 per manufacturer's protocol three days after treatment.

254 To assess cell proliferation and viability by crystal violet staining, 25,000 (HCC1806 and
255 BT-549) or 50,000 (MDA-MB-453 and MDA-MB-468) cells were plated per well of a 6-well dish.
256 The cells were treated as indicated one day following plating. Cells were washed with 1x PBS
257 and fixed in 100% methanol after seven to fourteen days of growth, depending on the cell line.
258 The cells were then stained with 0.005% Crystal Violet solution containing 25% methanol
259 (Sigma-Aldrich), prior to washing with water and imaging using a ChemiDoc Imaging System
260 (Bio-Rad). Percent stained area was measured using Fiji (ImageJ).

261 **Cellular A-to-I Editing Analysis**

262 Cells were treated with DMSO or ZYS-1 for 48 hours prior to RNA harvesting and
263 purification using the Nucleospin RNA kit (Macherey-Nagel). cDNA was made from isolated
264 RNA using LunaScript Supermix (NEB). Sections around the A-to-I editing sites in ZDHHC20,
265 BPNT1, and MRPS16 were amplified using PrimeSTAR Max DNA Polymerase (Takara Bio) and
266 the primers listed in Table S1. PCR products were then resolved by agarose gel electrophoresis
267 and purified by the Monarch Gel Extraction kit (New England Biolabs). Purified products were
268 Sanger sequenced by Azenta with the primers listed in Table S1. The QSVAnalyzer program
269 was used to measure the peak heights of each A-to-I editing site. Percent editing was found by
270 dividing the edited base (G or C) peak height by the sum of the edited and unedited (A or T)
271 peak heights and multiplying by 100. The primer used to sequence the regions around the
272 ZDHHC20 and MRPS16 editing sites yielded the antisense sequence of this region; percent
273 editing for these sites was determined using C (edited) and T (unedited) peak heights.

274 **In Vitro A-to-I Editing Assay**

275 A plasmid encoding a portion of the 5-HT_{2C} mRNA was synthesized by Twist Bioscience.
276 This pTwist-5HT plasmid was linearized by KpnI restriction enzyme digest and purified by
277 agarose gel electrophoresis as described above. The 5-HT_{2C} RNA was in vitro transcribed using
278 HiScribe T7 Quick High Yield RNA (New England Biolabs). The in vitro transcribed RNA was
279 purified using the Monarch Spin RNA Cleanup kit (New England Biolabs) and the quality of the
280 RNA was assessed by denaturing polyacrylamide gel electrophoresis. The RNA was annealed
281 in template annealing buffer (10 mM Tris-HCl pH 7.5, 1 mM EDTA, and 100 mM NaCl) by
282 heating to 95 °C and cooling slowly to room temperature.
283 The in vitro A-to-I editing assay was modified from those used by the laboratory of Peter
284 Beal, University of California Davis (Mendoza et al. 2023). In vitro editing assays were carried
285 out in 10 µL reactions consisting of 1X ADAR1 reaction buffer (15 mM Tris pH 7.4, 26 mM KCl,
286 1.5 mM EDTA, 0.003% NP-40, 4% glycerol and 40 mM potassium glutamate), 0.5 mM DTT, 1
287 µg/mL yeast tRNA (Invitrogen), 0.16 U/µL RNase Inhibitor Murine (New England Biolabs), 4 nM
288 5-HT_{2C} RNA, 5 µM RT_primer (Table S1), 1 mM dNTPs and water to 8 µL. To this reaction mix,
289 DMSO or ZYS-1 dissolved in DMSO was added prior to initiating the reaction by addition of 200
290 nM ADAR1-p150 (BPS Bioscience). The reaction was incubated at 30 °C for 15 minutes for
291 ADAR1-p150 lot #231010-1 or 1 hr for lot #250218. The reaction was stopped by heating to 95
292 °C for 5 minutes. Reverse transcription followed immediately by the addition of ProtoScript II
293 Buffer to 1X final (New England Biolabs), DTT to 10.25 mM final, 200 U ProtoScript II Reverse
294 Transcriptase (New England Biolabs), 8 U RNase Inhibitor Murine and water to 20 µL total. The
295 samples were incubated at 25 °C for 5 minutes, 42 °C for 1 hour and 65 °C for 5 minutes. The
296 cDNA was cleaned using the Monarch PCR and DNA Cleanup kit. PrimeSTAR Max DNA
297 Polymerase was used to PCR amplify the cDNA using primers EA_F and EA_R, described in
298 Table S1. The PCR products were purified by agarose gel electrophoresis and Sanger
299 sequenced using the EA_F primer. A-to-I editing was quantified as described above.
300 **Quantitative PCR**

Total RNA isolation and cDNA synthesis was performed as above. Quantitative PCR (qPCR) was performed with Luna Universal qPCR MasterMix (NEB) on a QuantStudio3 system (Thermo Scientific). The primers used are listed in Table S1. For each primer, the amplification efficiency was verified to be within 90-110% allowing 'Fold Change' determination via the ΔΔCt. The geometric mean Ct of EEF1A1 and HSPA5 was used for normalization.

Data Availability Statement

All analysis scripts are available at (https://github.com/cottrellka/Smoak_et_al_2025). Dependency data (DepMap_Public_24Q4+Score, Chronos, and Achilles+DRIVE+Marcotte, DEMETER2) were acquired from the DepMap portal (https://depmap.org/portal/download/custom/, RRID:SCR_017655).

Acknowledgements:

This work was supported by R00MD016946 (K.A. Cottrell), the Purdue Institute for Cancer Research (start-up funding) NIH grant P30CA023168, and start-up funding from Purdue University Department of Biochemistry and College of Agriculture.

Author Contributions

K.A.C. and C.N.S. conceived the project. K.A.C. and C.N.S. designed the experiments. C.N.S., E.N.G., R.N.C., and K.A.C. performed the experiments. C.N.S. and K.A.C. performed the data analysis. K.A.C. and C.N.S. wrote the manuscript. All authors edited the manuscript.

Declaration of interests

The authors declare no competing interests.

323 **References**

324 Bass BL, Weintraub H (1988) An unwinding activity that covalently modifies its double-stranded
325 RNA substrate. Cell 55 (6):1089-1098. doi:10.1016/0092-8674(88)90253-x
326 Broad D (2024) DepMap 24Q4 Public. doi:10.25452/figshare.plus.27993248.v1
327 Burns CM, Chu H, Rueter SM, Hutchinson LK, Canton H, Sanders-Bush E, Emeson RB (1997)
328 Regulation of serotonin-2C receptor G-protein coupling by RNA editing. Nature 387
329 (6630):303-308. doi:10.1038/387303a0
330 Chow RD, Wang G, Ye L, Codina A, Kim HR, Shen L, Dong MB, Errami Y, Chen S (2019) In
331 vivo profiling of metastatic double knockouts through CRISPR-Cpf1 screens. Nat
332 Methods 16 (5):405-408. doi:10.1038/s41592-019-0371-5
333 Chung H, Calis JJA, Wu X, Sun T, Yu Y, Sarbanes SL, Dao Thi VL, Shilvock AR, Hoffmann HH,
334 Rosenberg BR, Rice CM (2018) Human ADAR1 Prevents Endogenous RNA from
335 Triggering Translational Shutdown. Cell 172 (4):811-824.e814.
336 doi:10.1016/j.cell.2017.12.038
337 Cottrell KA, Andrews RJ, Bass BL (2024a) The competitive landscape of the dsRNA world. Mol
338 Cell 84 (1):107-119. doi:10.1016/j.molcel.2023.11.033
339 Cottrell KA, Ryu S, Pierce JR, Soto Torres L, Bohlin HE, Schab AM, Weber JD (2024b)
340 Induction of Viral Mimicry Upon Loss of DHX9 and ADAR1 in Breast Cancer Cells.
341 Cancer Res Commun 4 (4):986-1003. doi:10.1158/2767-9764.CRC-23-0488
342 Cottrell KA, Torres LS, Dizon MG, Weber JD (2021) 8-azaadenosine and 8-chloroadenosine are
343 not selective inhibitors of ADAR. Cancer Res Commun 1 (2):56-64. doi:10.1158/2767-
344 9764.crc-21-0027
345 Deng X, Sun L, Zhang M, Basavaraj R, Wang J, Weng YL, Gao Y (2025) Biochemical profiling
346 and structural basis of ADAR1-mediated RNA editing. Mol Cell 85 (7):1381-1394.e1386.
347 doi:10.1016/j.molcel.2025.02.017
348 Ding HY, Yang WY, Zhang LH, Li L, Xie F, Li HY, Chen XY, Tu Z, Li Y, Chen Y, Yang SY (2020)
349 8-Chloro-Adenosine Inhibits Proliferation of MDA-MB-231 and SK-BR-3 Breast Cancer
350 Cells by Regulating ADAR1/p53 Signaling Pathway. Cell Transplant
351 29:963689720958656. doi:10.1177/0963689720958656
352 Fisher AJ, Beal PA (2024) Structural perspectives on adenosine to inosine RNA editing by
353 ADARs. Mol Ther Nucleic Acids 35 (3):102284. doi:10.1016/j.omtn.2024.102284
354 Freund EC, Sapiro AL, Li Q, Linder S, Moresco JJ, Yates JR, Li JB (2020) Unbiased
355 Identification of trans Regulators of ADAR and A-to-I RNA Editing. Cell Rep 31
356 (7):107656. doi:10.1016/j.celrep.2020.107656
357 Gandhi V, Plunkett W (2002) Cellular and clinical pharmacology of fludarabine. Clin
358 Pharmacokinet 41 (2):93-103. doi:10.2165/00003088-200241020-00002
359 Gannon HS, Zou T, Kiessling MK, Gao GF, Cai D, Choi PS, Ivan AP, Buchumenski I, Berger
360 AC, Goldstein JT, Cherniack AD, Vazquez F, Tsherniak A, Levanon EY, Hahn WC,
361 Meyerson M (2018) Identification of ADAR1 adenosine deaminase dependency in a
362 subset of cancer cells. Nat Commun 9 (1):5450. doi:10.1038/s41467-018-07824-4
363 Hartner JC, Schmittwolf C, Kispert A, Müller AM, Higuchi M, Seeburg PH (2004) Liver
364 Disintegration in the Mouse Embryo Caused by Deficiency in the RNA-editing Enzyme
365 ADAR1*. Journal of Biological Chemistry 279 (6):4894-4902.
366 doi:https://doi.org/10.1074/jbc.M311347200
367 Heraud-Farlow JE, Walkley CR (2020) What do editors do? Understanding the physiological
368 functions of A-to-I RNA editing by adenosine deaminase acting on RNAs. Open Biol 10
369 (7):200085. doi:10.1098/rsob.200085
370 Hong H, An O, Chan THM, Ng VHE, Kwok HS, Lin JS, Qi L, Han J, Tay DJT, Tang SJ, Yang H,
371 Song Y, Bellido Molias F, Tenen DG, Chen L (2018) Bidirectional regulation of

372 adenosine-to-inosine (A-to-I) RNA editing by DEAH box helicase 9 (DHX9) in cancer.
373 Nucleic Acids Res 46 (15):7953-7969. doi:10.1093/nar/gky396
374 Hu SB, Heraud-Farlow J, Sun T, Liang Z, Goradia A, Taylor S, Walkley CR, Li JB (2023)
375 ADAR1p150 prevents MDA5 and PKR activation via distinct mechanisms to avert fatal
376 autoinflammation. Mol Cell 83 (21):3869-3884.e3867. doi:10.1016/j.molcel.2023.09.018
377 Ihlenfeldt WD, Bolton EE, Bryant SH (2009) The PubChem chemical structure sketcher. J
378 Cheminform 1 (1):20. doi:10.1186/1758-2946-1-20
379 Ishizuka JJ, Manguso RT, Cheruiyot CK, Bi K, Panda A, Iracheta-Vellve A, Miller BC, Du PP,
380 Yates KB, Dubrot J, Buchumenski I, Comstock DE, Brown FD, Ayer A, Kohnle IC, Pope
381 HW, Zimmer MD, Sen DR, Lane-Reticker SK, Robitschek EJ, Griffin GK, Collins NB,
382 Long AH, Doench JG, Kozono D, Levanon EY, Haining WN (2019) Loss of ADAR1 in
383 tumours overcomes resistance to immune checkpoint blockade. Nature 565 (7737):43-
384 48. doi:10.1038/s41586-018-0768-9
385 Kung C-P, Terzich ND, Ilagen MXG, Prinsen MJ, Kaushal M, Kladney RD, Weber JH, Mabry
386 AR, Torres LS, Bramel ER, Freeman EC, Sabloak T, Cottrell KA, Ryu S, Weber WM,
387 Maggi L, Shriver LP, Patti GJ, Weber JD (2025) ADAR1 Regulates Lipid Remodeling
388 through MDM2 to Dictate Ferroptosis Sensitivity. bioRxiv:2025.2001.2016.633410.
389 doi:10.1101/2025.01.16.633410
390 Kung CP, Cottrell KA, Ryu S, Bramel ER, Kladney RD, Bao EA, Freeman EC, Sabloak T, Maggi
391 L, Weber JD (2021) Evaluating the therapeutic potential of ADAR1 inhibition for triple-
392 negative breast cancer. Oncogene 40 (1):189-202. doi:10.1038/s41388-020-01515-5
393 Liddicoat BJ, Piskol R, Chalk AM, Ramaswami G, Higuchi M, Hartner JC, Li JB, Seeburg PH,
394 Walkley CR (2015) RNA editing by ADAR1 prevents MDA5 sensing of endogenous
395 dsRNA as nonself. Science 349 (6252):1115-1120. doi:10.1126/science.aac7049
396 Liu H, Golji J, Brodeur LK, Chung FS, Chen JT, deBeaumont RS, Bullock CP, Jones MD, Kerr
397 G, Li L, Rakiec DP, Schlabach MR, Sovath S, Growney JD, Pagliarini RA, Ruddy DA,
398 MacIsaac KD, Korn JM, McDonald ER (2019) Tumor-derived IFN triggers chronic
399 pathway agonism and sensitivity to ADAR loss. Nat Med 25 (1):95-102.
400 doi:10.1038/s41591-018-0302-5
401 Mannion Niamh M, Greenwood SM, Young R, Cox S, Brindle J, Read D, Nellåker C, Vesely C,
402 Ponting Chris P, McLaughlin Paul J, Jantsch Michael F, Dorin J, Adams Ian R, Scadden
403 ADJ, Öhman M, Keegan Liam P, O'Connell Mary A (2014) The RNA-Editing Enzyme
404 ADAR1 Controls Innate Immune Responses to RNA. Cell Reports 9 (4):1482-1494.
405 doi:https://doi.org/10.1016/j.celrep.2014.10.041
406 Matthews MM, Thomas JM, Zheng Y, Tran K, Phelps KJ, Scott AI, Havel J, Fisher AJ, Beal PA
407 (2016) Structures of human ADAR2 bound to dsRNA reveal base-flipping mechanism
408 and basis for site selectivity. Nat Struct Mol Biol 23 (5):426-433. doi:10.1038/nsmb.3203
409 Mendoza HG, Matos VJ, Park S, Pham KM, Beal PA (2023) Selective Inhibition of ADAR1
410 Using 8-Azanebularine-Modified RNA Duplexes. Biochemistry 62 (8):1376-1387.
411 doi:10.1021/acs.biochem.2c00686
412 Pestal K, Funk CC, Snyder JM, Price ND, Treuting PM, Stetson DB (2015) Isoforms of RNA-
413 Editing Enzyme ADAR1 Independently Control Nucleic Acid Sensor MDA5-Driven
414 Autoimmunity and Multi-organ Development. Immunity 43 (5):933-944.
415 doi:10.1016/j.immuni.2015.11.001
416 Polson AG, Crain PF, Pomerantz SC, McCloskey JA, Bass BL (1991) The mechanism of
417 adenosine to inosine conversion by the double-stranded RNA unwinding/modifying
418 activity: a high-performance liquid chromatography-mass spectrometry analysis.
419 Biochemistry 30 (49):11507-11514. doi:10.1021/bi00113a004
420 Ramírez-Moya J, Baker AR, Slack FJ, Santisteban P (2020) ADAR1-mediated RNA editing is a
421 novel oncogenic process in thyroid cancer and regulates miR-200 activity. Oncogene 39
422 (18):3738-3753. doi:10.1038/s41388-020-1248-x

Romano PR, Garcia-Barrio MT, Zhang X, Wang Q, Taylor DR, Zhang F, Herring C, Mathews MB, Qin J, Hinnebusch AG (1998) Autophosphorylation in the activation loop is required for full kinase activity in vivo of human and yeast eukaryotic initiation factor 2alpha kinases PKR and GCN2. Mol Cell Biol 18 (4):2282-2297. doi:10.1128/MCB.18.4.2282

Shi Z, Li J, Ding J, Zhang Y, Min W, Zhu Y, Hou Y, Yuan K, Sun C, Wang X, Shen H, Wang L, Liang SQ, Kuang W, Yang P (2025) ADAR1 is required for acute myeloid leukemia cell survival by modulating post-transcriptional Wnt signaling through impairing miRNA biogenesis. Leukemia 39 (3):599-613. doi:10.1038/s41375-024-02500-7

Sinigaglia K, Cherian A, Du Q, Lacovich V, Vukić D, Melicherová J, Linhartova P, Zerad L, Stejskal S, Malik R, Prochazka J, Bondurand N, Sedláček R, O'Connell MA, Keegan LP (2024) An ADAR1 dsRBD3-PKR kinase domain interaction on dsRNA inhibits PKR activation. Cell Rep 43 (8):114618. doi:10.1016/j.celrep.2024.114618

Stringer BW, Day BW, D'Souza RCJ, Jamieson PR, Ensbey KS, Bruce ZC, Lim YC, Goasdoué K, Offenhäuser C, Akgül S, Allan S, Robertson T, Lucas P, Tollesson G, Campbell S, Winter C, Do H, Dobrovic A, Inglis PL, Jeffree RL, Johns TG, Boyd AW (2019) A reference collection of patient-derived cell line and xenograft models of proneural, classical and mesenchymal glioblastoma. Sci Rep 9 (1):4902. doi:10.1038/s41598-019-41277-z

Wagner RW, Nishikura K (1988) Cell cycle expression of RNA duplex unwindase activity in mammalian cells. Mol Cell Biol 8 (2):770-777. doi:10.1128/mcb.8.2.770-777.1988

Wang Q, Miyakoda M, Yang W, Khillan J, Stachura DL, Weiss MJ, Nishikura K (2004) Stress-induced apoptosis associated with null mutation of ADAR1 RNA editing deaminase gene. J Biol Chem 279 (6):4952-4961. doi:10.1074/jbc.M310162200

Wang X, Li J, Zhu Y, Shen H, Ding J, Zeng T, Min W, Liang SQ, Huang L, Shi Z, Huang F, Yuan K, Kuang W, Ji M, Sun C, Hou Y, Wang L, Chen W, Jiang Y, Hao H, Xiao Y, Yang P (2025) Targeting ADAR1 with a small molecule for the treatment of prostate cancer. Nat Cancer 6 (3):474-492. doi:10.1038/s43018-025-00907-4

Wiederschain D, Wee S, Chen L, Loo A, Yang G, Huang A, Chen Y, Caponigro G, Yao YM, Lengauer C, Sellers WR, Benson JD (2009) Single-vector inducible lentiviral RNAi system for oncology target validation. Cell Cycle 8 (3):498-504. doi:10.4161/cc.8.3.7701

Wong SK, Sato S, Lazinski DW (2001) Substrate recognition by ADAR1 and ADAR2. RNA 7 (6):846-858. doi:10.1017/s135583820101007x

Young AA, Juhler IG, Pierce JR, Bohlin HE, Harper HA, Onishile DS, Chua RN, Liu ME, Gardner EN, Elzey BD, Cottrell KA (2025) PACT suppresses PKR activation through dsRNA binding and dimerization, and is a therapeutic target for triple-negative breast cancer. bioRxiv:2025.2005.2027.656288. doi:10.1101/2025.05.27.656288

Zhang M, Deng X, Gao Y, Wang J (2025) Re: Concerns Regarding the Validation of ZYS-1 as a Bona Fide ADAR1 Inhibitor. bioRxiv:2025.2003.2007.641892. doi:10.1101/2025.03.07.641892

Zipeto MA, Court AC, Sadarangani A, Delos Santos NP, Balaian L, Chun HJ, Pineda G, Morris SR, Mason CN, Geron I, Barrett C, Goff DJ, Wall R, Pellecchia M, Minden M, Frazer KA, Marra MA, Crews LA, Jiang Q, Jamieson CHM (2016) ADAR1 Activation Drives Leukemia Stem Cell Self-Renewal by Impairing Let-7 Biogenesis. Cell Stem Cell 19 (2):177-191. doi:10.1016/j.stem.2016.05.004

Zou T, Zhou M, Gupta A, Zhuang P, Fishbein AR, Wei HY, Capcha-Rodriguez D, Zhang Z, Cherniack AD, Meyerson M (2024) XRN1 deletion induces PKR-dependent cell lethality in interferon-activated cancer cells. Cell Rep 43 (2):113600. doi:10.1016/j.celrep.2023.113600

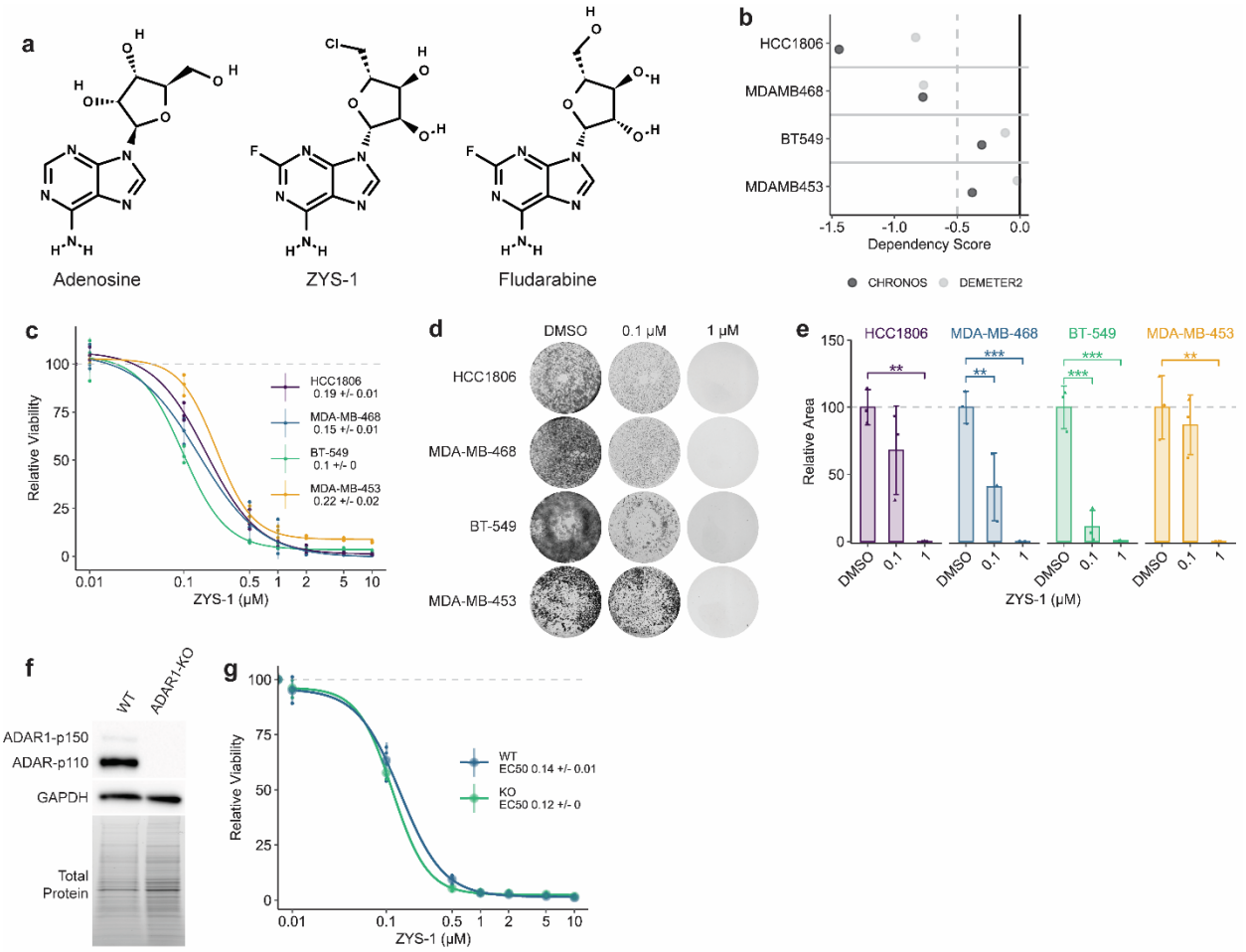

Figure 1: ZYS-1 is broadly cytotoxic to breast cancer cells, irrespective of ADAR1 expression or ADAR1-dependency.

a Structures of adenosine, ZYS-1, and fludarabine, made using PubChem Sketcher V2.4 (Ihlenfeldt et al. 2009). **b** CHRONOS and DEMETER2 ADAR1 dependency scores for relevant TNBC cell lines as evaluated using CRISPR-Cas9 knockout screening or RNAi screening, respectively (Broad 2024). A CHRONOS or DEMETER2 score below –0.5 indicates gene dependency (Broad 2024). **c** Dose-response evaluation of cell viability for ZYS-1 in cell lines given in **b**, as measured using the CellTiter-Glo 2.0 assay. Representative images (**d**) and quantification (**e**) of crystal violet staining following ZYS-1 treatment of cell lines given in **b**. **f** Immunoblot analysis of ADAR1 protein expression in WT and ADAR1-KO BT-549 cells. **g** Dose-response evaluation of cell viability for ZYS-1 in WT and ADAR1-KO BT-549 cells, as measured using the CellTiter-Glo 2.0 assay. For **c** and **g**, large points are the average of three biological replicates, and smaller points are the average of three technical replicates performed for each biological replicate. For **e**, bars indicate the average of three biological replicates. Error bars represent the average ± SD. Statistical analysis for **e** performed using one-way ANOVA with post-hoc Tukey. ** $p < 0.01$, *** $p < 0.001$.

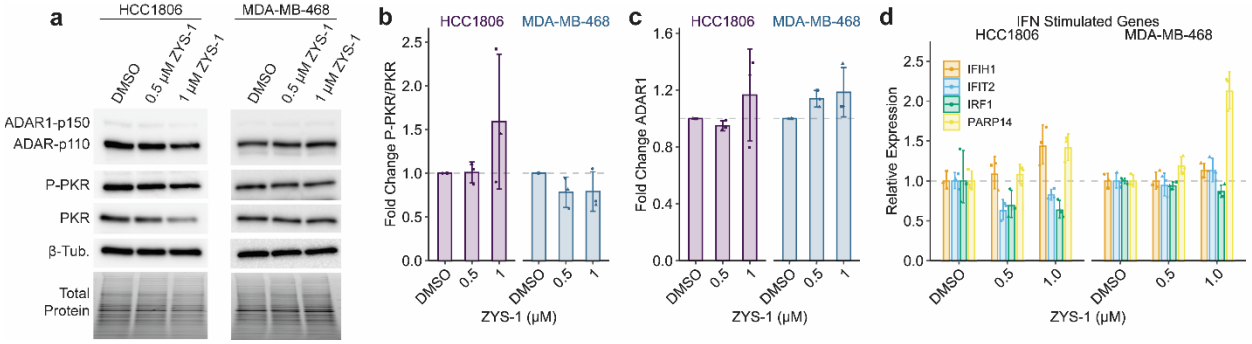

Figure 2: Treatment with ZYS-1 does not induce PKR activation or ISG expression. **a** Immunoblot analysis of PKR activation (P-PKR) in the ADAR1-dependent cell lines HCC1806 and MDA-MB-468 following treatment with ZYS-1. **b** and **c**, Quantification of the immunoblot shown in **a**. **d** qPCR analysis of IFN-stimulated gene expression in ZYS-1-treated HCC1806 and MDA-MB-468 cells. Bars indicate the average of three biological replicates. Error bars represent the average ± SD.

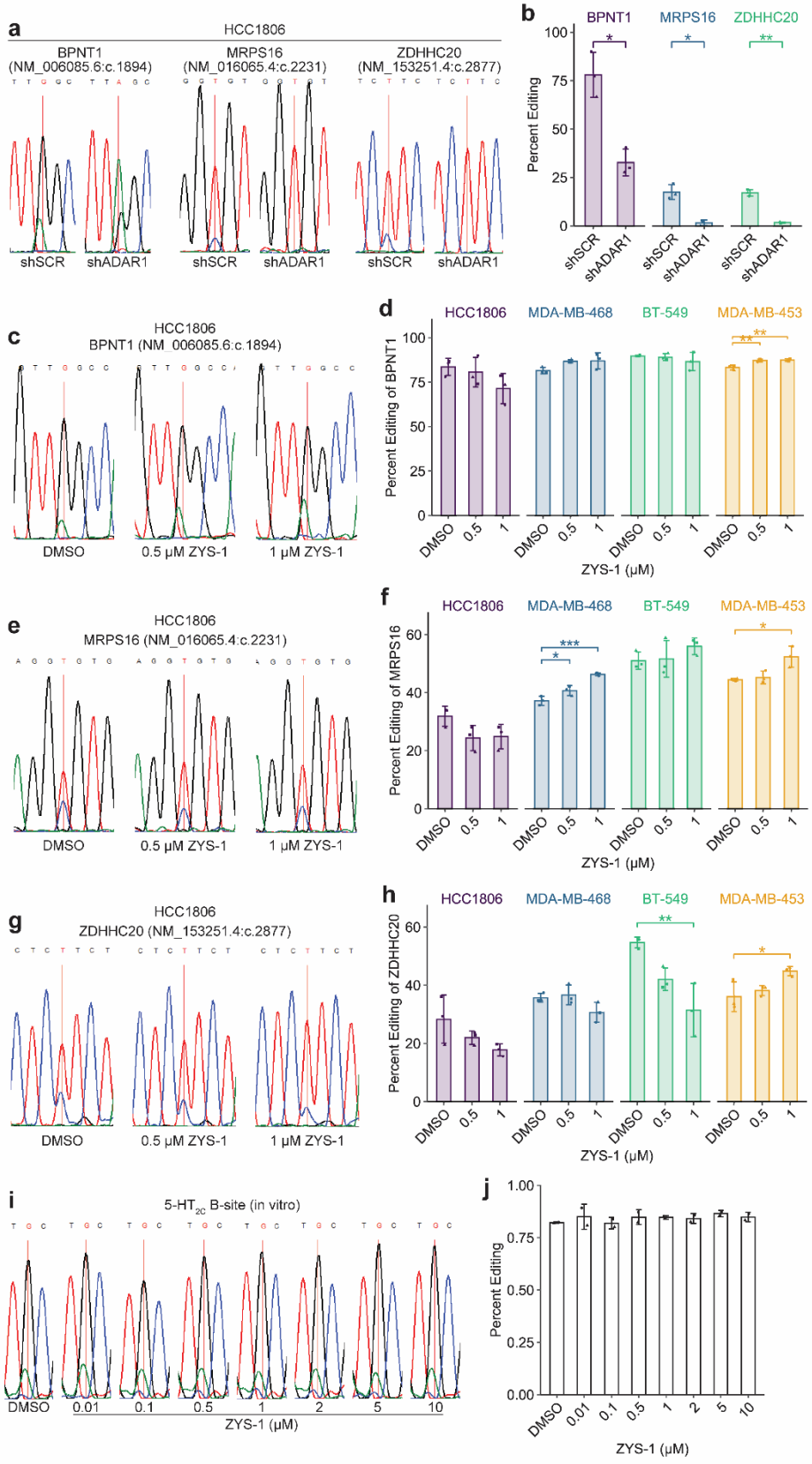
a
HCC1806
BPNT1 (NM_006085.6:c.1894)
MRPS16 (NM_016065.4:c.2231)
ZDHHC20 (NM_153251.4:c.2877)
shSCR
shADAR1
b
BPNT1
MRPS16
ZDHHC20
Percent Editing
c
HCC1806
BPNT1 (NM_006085.6:c.1894)
DMSO
0.5 μM ZYS-1
1 μM ZYS-1
d
HCC1806
MDA-MB-468
BT-549
MDA-MB-453
Percent Editing of BPNT1
ZYS-1 (μM)
e
HCC1806
MRPS16 (NM_016065.4:c.2231)
f
Percent Editing of MRPS16
g
HCC1806
ZDHHC20 (NM_153251.4:c.2877)
h
Percent Editing of ZDHHC20
i
5-HT2C B-site (in vitro)
j
Percent Editing

Figure 3

500 **Figure 3: ZYS-1 treatment does not inhibit A-to-I editing by cellular or recombinant**
501 **ADAR1.**
502 **a** Sanger sequencing trace of BPNT1, MRPS16, and ZDHHC20 editing sites in HCC1806
503 control or ADAR1 knockdown cells. **b** Quantification of percent editing using Sanger sequencing
504 results depicted in **a**. Representative Sanger sequencing trace of BPNT1 (**c**), MRPS16 (**e**), and
505 ZDHHC20 (**g**) editing sites in HCC1806 following treatment with ZYS-1. Percent editing
506 quantification of the BPNT1 (**d**), MRPS16 (**f**), and ZDHHC20 (**h**) transcripts using Sanger
507 sequencing in relevant TNBC cell lines. **i** Sanger sequencing trace of the 5-HT_{2C} B-site following
508 incubation with purified ADAR1 and ZYS-1 as indicated. **j** Quantification of B-site percent editing
509 using Sanger sequencing results depicted in **i**. For **a**, **c**, **e**, **g**, and **i**, sites that are edited by
510 ADAR1 are indicated by the red vertical line. Bars indicate the average of three biological
511 replicates (**b**, **d**, **f**, and **h**) or two experimental replicates (**j**). Error bars represent the average ±
512 SD. Statistical analysis performed using Student's t-test for **b** and one-way ANOVA with post-
513 hoc Tukey for **d**, **f**, and **h**. * $p < 0.05$, ** $p < 0.01$, *** $p < 0.001$.
514

515

516

517

518

519